Growth of Naphthalene Crystals from Supercritical CO_2 Solution

Clifford Y. Tai and Chuen-Song Cheng
Dept. of Chemical Engineering, National Taiwan University, Taipei, Taiwan 106, R.O.C.

The growth phenomena, mechanism, and kinetics of naphthalene crystals from supercritical CO_2 solution were studied by using a single-crystal technique. Distinct growth features were observed, including the development of individuals from the seeds and the sprouting of plates from the individuals. The surface integration proceeded by two-dimensional nucleation mechanism at face corners and by subsequent spreading of the nuclei. The measured growth rates as functions of supersaturation and solubility were consistent with the derived growth-rate equations, based on the corner nucleation mechanism. In comparison with crystal growth from conventional media, the growth of naphthalene crystals from supercritical CO_2 solution is similar to liquid-solution growth as far as growth mechanism and kinetics are concerned.

Introduction

Crystallization is conventionally conducted from the liquid solution, the vapor, and the melt. The process consists of nucleation events and the subsequent growth of nuclei. The growth process is important because it controls the crystal qualities, such as size distribution, habit, and purity. Various growth phenomena have been found and explained over the past decades. For example, crystals grow layerwise in most conditions to form crystals bounded by facets, and unstable growth of the facets leads to hopper faces (Chernov, 1984). Other notable growth phenomena include the development of individuals on spherical potassium alum crystals (Buckley, 1951) and the sprouting of plates from column snow crystals (Nakaya, 1954). Besides the growth phenomena, the growth mechanism and kinetics have also been well-developed. Burton et al. (1951) presented the famous BCF theory (Burton–Cabrera–Frank), in which they derived the growth rates of a crystal face growing from vapor phase due to parallel steps generated by a screw dislocation. In this theory, gas kinetics was incorporated to quantify the flux arriving at the crystal face. Bennema (1967a) then applied the BCF theory to interpret the growth rates of crystals growing from liquid solution by introducing the effect of solvation, which characterizes the liquid-solution growth. In contrast to the BCF theory, Chernov (1964) considered the kinetics of two-dimensional nucleation at a face corner and gave the formation time of a nucleus. More recent kinetic development was the two-step model (Tai and Lin, 1987; Tai et al., 1992), in which the overall growth process was separated into a bulk diffusion and a surface integration step connected in series.

Recently, crystallization from supercritical fluids has attracted much attention because of several advantages in comparison with conventional crystallization. First, it can produce nearly monosized fine crystals without temperature effect and impurity contamination (Paulaitis et al., 1983). Second, accurate control of crystal size is possible through small changes in process variables (Mohamed et al., 1989). Third, it provides an efficient method for separating solute mixtures (Kelley and Chimowitz, 1989). A further benefit is that no operation on solid–liquid separation and product drying is needed. The use of supercritical carbon dioxide to crystallize materials gains advantages over others, although several supercritical fluids can be applied. This is because carbon dioxide is inexpensive, nontoxic, nonflammable, and environmentally acceptable. Moreover, the low critical temperature of carbon dioxide (31°C) permits crystallizing fine chemicals and pharmaceuticals at moderate temperatures with minimal thermal degradation. Further, the critical pressure (73.8 bar) is not too high to result in an unacceptable investment in equipment. A few studies on crystallization from supercritical carbon dioxide have been published in the literature. Krukonis (1984) first explored a novel RESS (rapid expansion of supercritical solutions) process for producing very fine crystals, and much work has been done to characterize the

Correspondence concerning this article should be addressed to C. Y. Tai.

process since. For example, Larson and King (1986) and Mohamed et al. (1989) showed that the naphthalene crystals produced by this method retained the crystallinity of the virgin crystals; Mohamed et al. (1989) and Berends et al. (1993) reported that the pre- and postexpansion conditions influenced the sizes of the precipitated crystals; Shaub et al. (1991) found that the geometry of the expansion nozzle was also effective in determining the crystal sizes. Further information on the RESS process can be found in the review article by Tom and Debenedetti (1991). In contrast to the studies on the RESS process, Tavana and Randolph (1989) developed a technique of batch crystallization to study the crystallization mechanism from supercritical carbon dioxide. In the study, they confirmed the validity of the conventional concept that crystals are formed by nucleation and subsequent growth. On this basis, Debenedetti (1990) has studied the homogeneous nucleation of crystals from supercritical carbon dioxide. However, no systematic work has been done, so very little is known up to now about the growth of crystals from the supercritical fluid.

The purpose of this study was to explore the phenomenon, mechanism and kinetics of crystal growth from supercritical CO_2 solution, and to see if they were similar to those from liquid solution and from vapor phase. A single-crystal technique was developed to observe the growth phenomena and to measure the growth rates of naphthalene crystals from supercritical CO_2 solution. The growth mechanism was inferred from the observed phenomena, and the corresponding growth rate equations were derived to interpret the measured growth rates.

Growth Kinetics from Supercritical Fluids

The growth rates of crystals from supercritical fluids depend on temperature, pressure, and solute concentration when neglecting hydrodynamic and impurity effects, that is,

$$R = f(T, P, C), \tag{1}$$

where R is the crystal growth rate, T is the system temperature, P is the system pressure, and C is the solute concentration. Equation 1 can be rewritten as

$$R = f(T, C_e, C) \tag{2}$$

by eliminating the pressure term using the fact that $C_e = f(T, P)$. Equation 2 means that solubility acts independently as does solute concentration and temperature, to affect the growth rate. This contradicts the kinetics of crystal growth from liquid solution, where solubility is not independent of temperature.

The effects of solubility and solute concentration on growth rate can be derived by considering the details of a growth process. The growth of a crystal face is mainly controlled by the adsorption and desorption of solute onto and from the crystal face. The growth rate thus can be expressed in terms of the net adsorption rate of solute onto the face:

$$R = (\Omega/A_t)\int_{A_t} (J_a - J_d)\quad dA, \tag{3}$$

where Ω is the molar volume of the crystal, A_t the total area of the crystal face, J_a the adsorption flux of the solute, and J_d the desorption flux of the solute. Assuming that the adsorption flux J_a is uniform over the crystal face, Eq. 3 can be rewritten as

$$R = [\Omega(J_a - J_e)/A_t]\int_{A_t} [1-(J_d - J_e)/(J_a - J_e)]\quad dA, \tag{4}$$

where J_e is the value of J_a or J_d at equilibrium condition. Equation 4 can be further advanced by taking $J_a = K_a C$ (Strickland-Constable, 1968) and $J_d = n/\tau_s$ (Burton et al., 1951), where K_a is the adsorption rate constant, and n and τ_s are the concentration and mean life of the adsorbed solute, respectively. The result is

$$R = K_a \Omega C_e \sigma \int_{A_t} (1 - \sigma_s/\sigma)\quad d(A/A_t), \tag{5}$$

where σ is the bulk supersaturation and σ_s is the local surface supersaturation, defined as $\sigma = (C/C_e) - 1$ and $\sigma_s = (n/n_e) - 1$. Note that the equivalence $J_e = K_a C_e = n_e/\tau_s$ has been used in deriving Eq. 5, which establishes the effects of solute concentration (expressed in terms of bulk supersaturation) and solubility on the growth rate.

Equation 5 is composed of a nonintegration part $K_a \Omega C_e \sigma$ and an integration part. The terms in the nonintegration part are all measurable except K_a. The integration part involves the distribution of σ_s over the crystal face, which depends on the step structure of the crystal face and cannot be generally obtained. Physically, the nonintegration part represents the limiting growth rate when the surface-diffusion and step-incorporation barriers of the adsorbed solute molecules are negligible and result in zero σ_s all over the crystal face (Burton et al., 1951). The integration part ($\leqq 1$) corrects the effect of nonzero σ_s when the two barriers are important. Equation 5 is valid for liquid-solution growth, although it is derived for growth from supercritical fluids. However, solubility is usually lumped with other crystal properties to form a rate constant in liquid-solution growth because it is always coupled with temperature and conventionally regarded as one crystal property pertaining to temperature.

To correlate the growth rate with supersaturation for the crystal faces that grow, as described by Chernov (1964), by the spreading of equidistant steps generated by two-dimensional nucleation at the face corners, Eq. 5 is integrated by substituting the distribution of σ_s for a crystal face composed of equidistant steps (Burton et al., 1951). The result is

$$R = \beta K_a \Omega C_e \sigma (2x_s/y_0) \tanh(y_0/2x_s), \tag{6}$$

where β is a factor representing the step-incorporation barrier, y_0 the distance between two adjacent steps, and x_s the mean diffusion length of the adsorbed solute molecules. The further advance of Eq. 6 involves correlating y_0 and σ. To achieve this, y_0 is first expressed as

$$y_0 = v\tau, \tag{7}$$

where v is the step velocity and τ the period of forming a two-dimensional nucleus at a face corner. Then, a derivation of v similar to that by Burton et al. (1951) gives

$$v = \beta K_a \Omega C_e \sigma (2x_s/d) \tanh(y_0/2x_s), \tag{8}$$

where d is the step height. Finally, τ is given as (Chernov, 1964)

$$\tau = \phi v^{-2/3} \exp[B/\ln(1+\sigma)], \tag{9}$$

where ϕ is a constant and B is equal to $1.33(\gamma/kT)^2$ (γ is the edge free energy). In principle, y_0, v, and τ can be solved by using Eqs. 7 to 9, and growth rate can be correlated with supersaturation by simply substituting y_0 into Eq. 6. However, no general analytical solution is possible due to the nonlinearity of the equations. Instead, the solutions for two limiting cases are derived. In one case, supersaturation and thus nucleation rate are so low that y_0 is much larger than $2x_s$. The solution of the growth rate for this case is

$$R = \alpha C_e^{2/3} \sigma^{2/3} \exp[-B/\ln(1+\sigma)], \tag{10}$$

where α is equal to $(2\beta K_a \Omega x_s d^{1/2})^{2/3}/\phi$. According to Eq. 10, a plot of $\ln(R/\sigma^{2/3})$ vs. $1/\ln(1+\sigma)$ would give a straight line with the slope equal to the negative value of B. In the other case, supersaturation and nucleation rate are so high that y_0 is much less than $2x_s$. The solution for this case is easy, that is,

$$R = \beta K_a \Omega C_e \sigma. \tag{11}$$

A plot of R/C_e vs. σ for the data taken at various solubilities with the temperature kept constant would give a straight line with the slope equal to $\beta K_a \Omega$. Note that Eq. 11 is equivalent to $R = (\beta \Omega n_e/\tau_s)\sigma$, which is the linear law of the BCF theory (Burton et al., 1951). Also, Eq. 11 is equivalent to $R = K\Delta C$ ($K = \beta K_a \Omega$ and $\Delta C = C_e \sigma$), which has been applied to many systems for crystal growth from liquid solution.

Experimental

The growth phenomena were observed and the growth rates were measured at a temperature of 45°C. Other operating variables such as pressure, supersaturation, and the superficial velocity of solution were varied to study their effects. Solubilities were also measured at various levels of temperature and pressure because they were needed in the determination of bulk supersaturation.

Apparatus and seed crystals

The apparatus for this study was a modified version of the setup for growing crystals from liquid solution (Tai et al., 1992). The constructed system was allowed to observe growth phenomena and to measure growth rates *in situ*. It was also allowed to measure the solubilities of solid materials in supercritical carbon dioxide.

The apparatus, shown in Figure 1, was mainly a closed loop consisting of a growth cell for growing crystals, an extractor

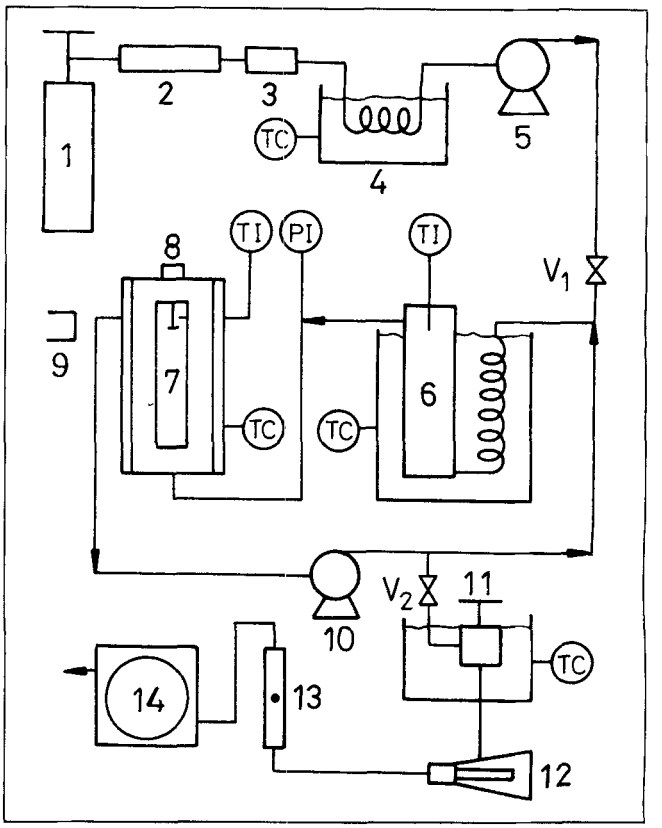

Figure 1. Experimental apparatus.

(1) CO_2 cylinder; (2) silica-gel bed; (3) filter; (4) cooler; (5) feeding pump; (6) extractor; (7) crystal growth cell; (8) needle to fix seed crystal; (9) microscope; (10) circulation pump; (11) expansion valve; (12) crystal collector; (13) flowmeter; (14) wet test meter. PI = pressure indicator; TI = temperature indicator; TC = temperature controller.

an extractor for supplying solute, and a pump for circulating solution. The extractor was immersed in a water bath for temperature control. A crystal bed (1.8 cm × 25 cm) of ground naphthalene (Wako, reagent grade) was packed in the extractor. The growth cell was a modified liquid level gauge (Jerguson, Model 18-T-30) with a jacket to permit temperature regulation. In the cell, a needle holding a seed crystal of about 1.5 mm was screwed in. The circulation pump was a Milton Roy Minipump or a Clark-Cooper Model for low or high circulation rates, respectively. Both pumps were of the variable-stroke, dual-piston type. The pipeline of the closed loop was built of 1/4-in.-OD stainless-steel tubes. Total volume of the closed loop was about 350 cm^3.

Seed crystals of naphthalene were prepared from ethanol solution. Naphthalene crystals, obtained by evaporating a drop of dilute solution, were introduced into a slightly supersaturated solution at room temperature to induce nucleation. The induced nuclei were allowed to grow in the solution without stirring. Seed crystals so obtained were bounded by {001}, {20$\bar{1}$}, and {110} faces; the same as those reported by Wells (1946) in morphology.

Crystal growth experiments

The procedure for conducting crystal growth experiments was as follows. Liquid carbon dioxide, 99% pure, was first

passed through a silica-gel bed to remove possible water moisture, and then through a precooler for preventing possible vaporization. Finally, it was delivered into the closed loop by a piston pump (Milton Roy Minipump) until the desired pressure, monitored by a digital gauge (Heise, Model 901A) and controlled to within ± 0.3 bar, was reached. Meanwhile, the temperature levels in the extractor and in the growth cell, measured by a Marlin thermometer (the detectors Model PRT4 and the indicator Model 410A) and controlled to within ± 0.1°C, were adjusted to a same desired value, which was less than 45°C in all runs. Also, the solution in the closed loop was circulated at the desired rate, which was calibrated beforehand. As the circulation proceeded, the concentration of solute gradually approached a saturation value equal to the solubility corresponding to the system pressure and the extraction temperature. Saturation was guaranteed when no dissolution of the seed crystal was detected by a microscope (Nikon, Model SMZ-10, 80×) within one-half hour. A circulation time of 0.5 to 2 hours was needed to achieve saturation at circulation rates of 7.5 to 300 cm^3/min. Generally, longer circulation time was needed at a lower circulation rate. After saturation, the solution in the growth cell was heated to 45°C with no rise of pressure by releasing a small volume of the solution. The solution therefore became supersaturated by raising the temperature, because our system was operated in the retrograde region where higher temperature causes lower solubility. Then, the seed crystal was allowed to grow. The growth phenomena were observed and the growth rates were measured by using the microscope, which was equipped with a camera and a micrometer on the eyepiece.

Growth rates were obtained by the displacement of a growing face using a linear regression analysis. Supersaturation was estimated by the difference between the solubilities corresponding to the levels of temperature in the extractor and in the growth cell at the operating pressure. Solubilities were expressed in grams of solute per 100 g of solvent, as is usual for crystal growth from liquid solution.

Two difficulties were encountered in operating the system. First, at a circulation rate as low as 7.5 cm^3/min and a system pressure higher than 95 bar, seed crystals would be completely dissolved before the solution became saturated. Second, at high circulation rates, under which the complete dissolution of seed crystals no longer happened, heterogeneous nucleation at cell outlet caused gradual blockage, which jeopardized the long-range operation.

Measurement of solubilities

The procedure for measuring solubilities was almost the same as that of growth experiments. Carbon dioxide was delivered into and circulated in the closed loop to achieve saturation. Then the saturated solution was expanded through a micrometering valve (Autoclave Engineers, Model 30 VRMM), and immersed in a water bath of 80°C. After being separated from the precipitated crystals in a collector, the carbon dioxide gas stream passed through a wet test meter (Shinagawa, Model WK-2B) and its total volume was measured. Upon the completion of an experiment, solubility was determined by the weight loss of the packed solute and the mass of the released carbon dioxide.

Table 1. Constants and Parameters in Eq. 12 at Various Levels of Pressure

P (bar)	T_0 (°C)	C_{e0} (g/100 g)	a	b
76.9	45.0	0.169	4.149×10^{-5}	4.092
83.8	46.2	0.276	1.217×10^{-2}	2.046
90.7	45.6	0.493	1.260×10^{-1}	1.342

Results and Discussion

Solubility

An empirical correlation between solubility and temperature at a given pressure was represented by

$$\ln(C_e/C_{e0}) = a(T_0 - T)^b, \tag{12}$$

where T_0 is the chosen reference temperature, and C_{e0} the corresponding solubility. The constants and parameters were summarized in Table 1 at three levels of pressure. The solubilities at 45°C obtained in this experiment matched those reported by Tsekhanskaya et al. (1964) to within $\pm 10\%$.

Growth phenomena and mechanism

The growth of a naphthalene seed in the supercritical CO_2 solution showed two distinct features as seen in Figure 2. First, many small individual crystals with light-reflecting faces developed on the seed crystal, which had been partly dissolved to become a hemiellipsoid before the solution became saturated. Second, plates sprouted from some of the individuals that located away from the pole of the hemiellipsoid. The first feature occurred regardless of the operating conditions. In contrast, the second feature was observed under specific conditions; pressure, solution velocity, and supersaturation were all influential. At a pressure of 83.8 bar and a

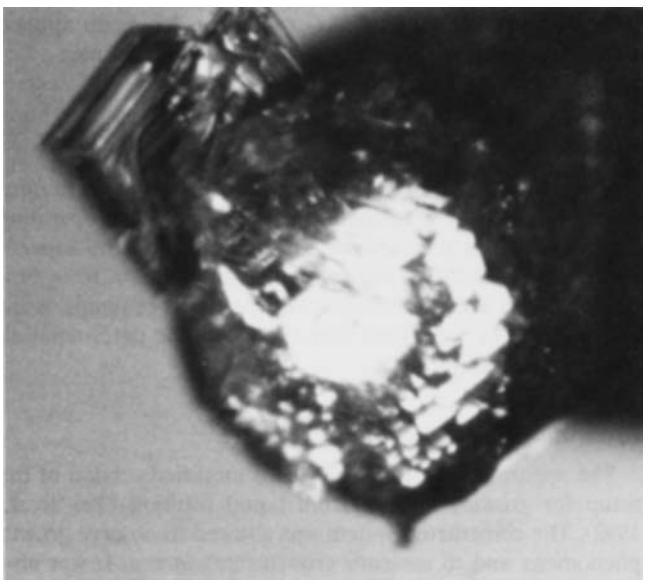

Figure 2. Growing naphthalene crystal at 318 K and 83.8 bar with supersaturation of 0.028 and solution velocity of 2.4×10^{-4} m/s.

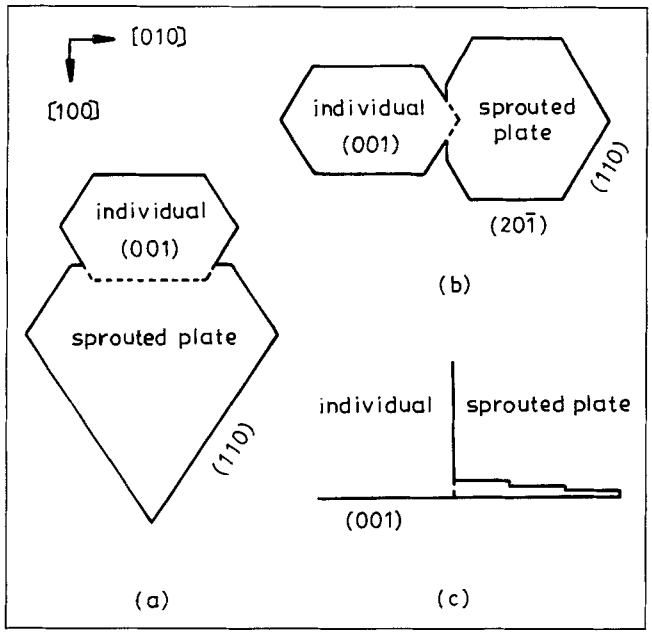

Figure 3. Sprouting of plate from an individual.

(a) Sprouting in the [100] direction. (b) Sprouting in the [010] direction. (c) Side view of the sprouted plate.

Figure 4. Hopper structure on the flat basal face of a sprouted plate.

The face has been coated by a thin layer of lacquer to reveal its topography.

solution velocity of 2.4×10^{-4} m/s, the plate sprouting was observed within the whole operable supersaturation range, that is, from 0.028 to 0.40. However, supersaturation became effective when the solution velocity or pressure was varied. At the same pressure, but with higher solution velocities between 1.2 and 9.4×10^{-3} m/s, a critical level of supersaturation of about 0.18 was found, above which the plate sprouting could be observed. On the other hand, at a solution velocity of 2.4×10^{-4} m/s, but with a higher pressure of 90.7 bar or with a lower pressure of 76.9 bar, the plate sprouting occurred randomly, and thus the effect of supersaturation was not conclusive.

The (001) faces of the individuals underwent facet growth at small sizes and turned into hopper growth when they grew larger. The facet growth was manifested by the light-reflecting faces, which appeared regardless of the operating conditions. In contrast, the hopper growth was assured by the appearance of hopper faces consisting of macrosteps. Critical sizes for the hopper growth were in the range of about 3 to 7×10^{-4} m, depending on the supersaturation and solution velocity. A higher supersaturation and lower solution velocity rendered the critical size smaller.

The plates might sprout in the [100] or in the [010] direction, as shown in Figure 3. Often the sprouting occurred in the [100] direction, resulting in truncated rhombic plates, but occasionally it occurred in the [010] direction, resulting in a truncated hexagonal plate. The rhombic plates were bounded by basal {001} faces and lateral {110} faces, while the hexagonal plates contained additional lateral {20$\bar{1}$} faces.

Different topographies were found on the two basal (001) faces of a plate regardless of the operating conditions; one was flat and the other was stepped (Figure 3c). The flat face was usually smooth, but a hopper structure occasionally appeared. Figure 4 shows a half-broken hopper. The stepped face was structurally complex, with a key feature of step trains, which were separated by a ridge lying on the long diagonal of the rhombic plate, as shown in Figure 5. A step might decompose into several steps that lessened step height and reduced the distance between steps. Consequently, the step height and distance between steps were varied on a plate. However, the step height was in the order of 10^{-5} m, and the distance between steps was less than 10^{-4} m. The features of the stepped basal faces became different when the lateral growth of plates was too fast; the ridge disappeared, and the step height diminished. A rough estimate of the critical rate was 2×10^{-6} m/s.

A lateral (110) face might grow stably, or unstably to become zigzag or dendritic, as shown in Figure 6 (see the lower

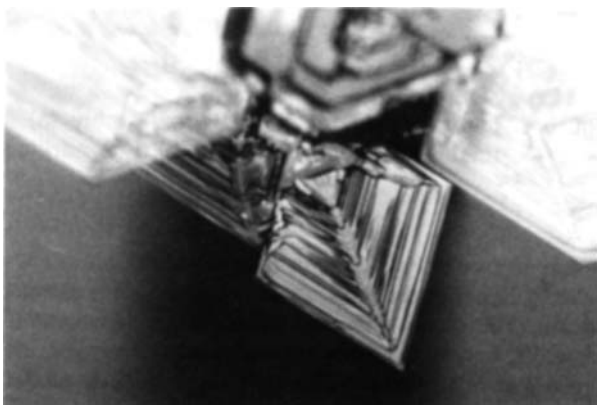

Figure 5. Topography of the stepped basal face of a sprouted plate.

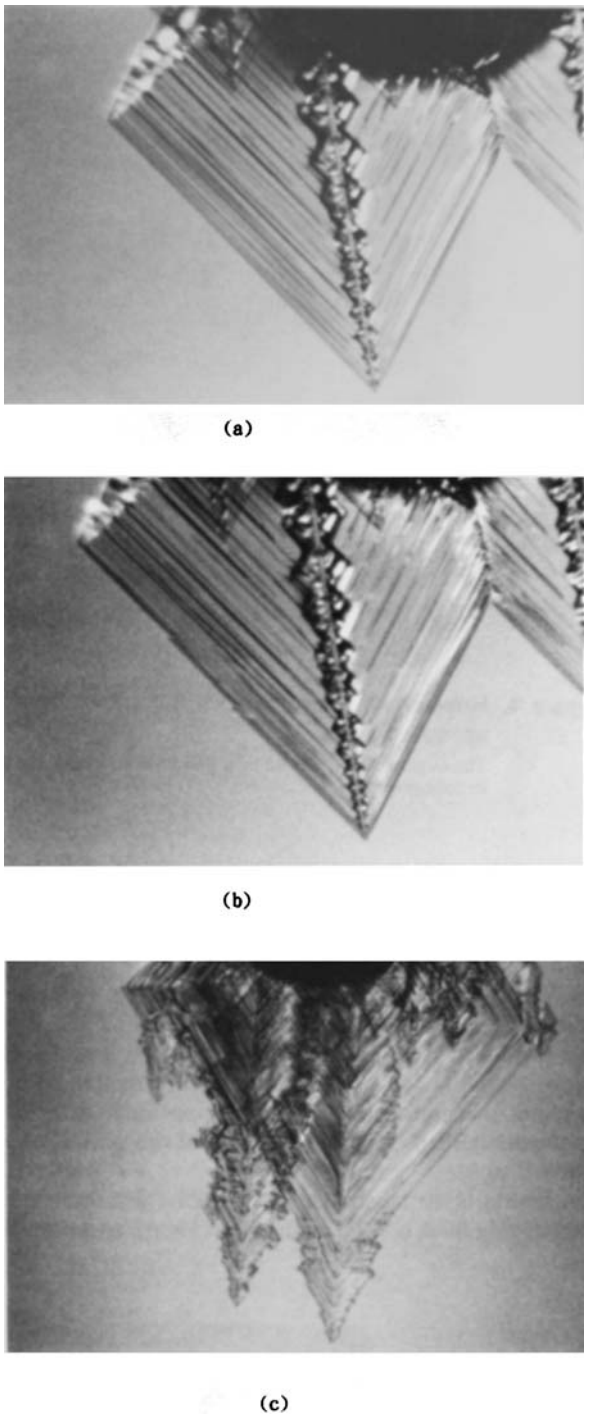

Figure 6. Lateral (110) faces that grew stably (a) and unstably to become zigzag (b) or dendritic (c).

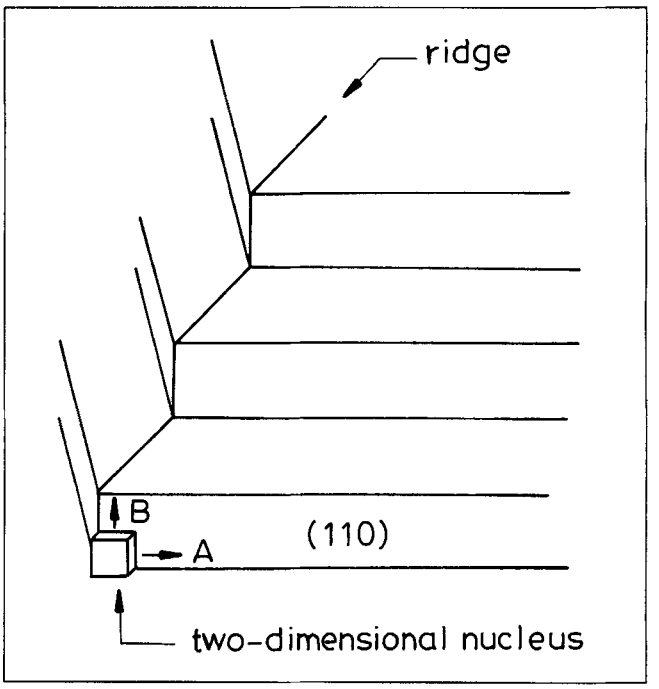

Figure 7. Mechanism of corner nucleation for the growth of lateral (110) faces.

The structure along the ridge has been neglected.

left lateral face in Figure 6b for zigzags). Supersaturation was found to influence the growth stability, while solution velocity did not. The plates grew stably at relative supersaturation below 0.1, but dendritic growth occurred sooner or later on all plates at relative supersaturation above 0.25. At moderate supersaturation between these two values, a few lateral faces of the plates became zigzag. The length of the lateral faces also seemed important for growth stability, because the lateral faces grew unstably only when the size was above 10^{-3} m.

The growth mechanism of the (001) faces of the individuals can be inferred from the growth phenomena, facet growth at small size, and hopper growth at large size, by applying the theory of Chernov (1984) for the stability of polyhedral crystals. According to the theory, both the surface integration mechanism and bulk-diffusion barrier are determinant factors for the stability of a crystal face. Facet growth results from the environment of the negligible bulk-diffusion barrier, regardless of the surface integration mechanism, and hopper growth from that of the important bulk-diffusion barrier, together with the surface integration mechanism of two-dimensional nucleation at the face corners. The theory also shows that crystals tend to grow in the kinetic regime at a small size, which results in a facet, and in the diffusion regime at a large size, which results in a hopper. Moreover, the theory predicts that the critical size of hopper growth decreases with supersaturation and increases with solution velocity. Our observation on facet and hopper growth was consistent with the theory. Thus it can be concluded that the corner nucleation mechanism exists in our system, and that the bulk-diffusion barrier is unimportant at small sizes but important at large sizes.

The lateral (110) faces may grow by the corner nucleation mechanism, as shown in Figure 7. This mechanism explains the formation of the stepped basal faces and the stability of the lateral faces. Nuclei first formed at the tip and then spread in the A and B directions. Stepped basal faces resulted if the spreading rates were fast in the A direction but slow in the B direction. Unstable growth of the lateral faces arose when the spreading rates in the A direction were somehow de-

layed. The low spreading rates in the B direction are probably intrinsic for the system and are related to the surface diffusion process. In contrast, the delay in the A direction likely occurs occasionally, and is determined by the fluctuation of supersaturation. The occurrence of stable, zigzag, and dendritic lateral faces at small, moderate, and high supersaturation, respectively, can be understood if the fluctuation varied with the level of supersaturation. The fluctuation was too minor to cause any delay at low supersaturation, so the lateral faces grew stably. The delay was slight at moderate supersaturation, resulting in the zigzag lateral faces, but became significant at high supersaturation, where the dendritic lateral faces formed. The proposition of supersaturation fluctuation to influence the growth of the lateral faces was evidenced by the fact that some plates grew stably while others grew unstably in the same apparent environment. Further signs were that a zigzag face sometimes recovered and became stable, and that a dendritic face often became flat on the part near the tip of the plate.

Growth kinetics

The growth rates of the (001) faces of the individuals were measured with the (001) faces perpendicular to the solution flow. Among the developing individuals on a seed crystal, the one that sprouted no plate was chosen for measurement. A displacement-time plot showed that the growth rates were initially constant and tended to decrease gradually. The initial growth rates, according to Chernov's analysis (1984), corresponded to the kinetic-regime growth, where the growth rates were determined almost completely by the surface integration process. The decreasing rates resulted from an increased bulk-diffusion barrier when the individuals grew larger. This confirmed the previous conclusion that the bulk-diffusion barrier for individuals was unimportant at small sizes but important at large sizes. The initial constant growth rates varied from 3.3×10^{-9} to 9.3×10^{-8} m/s, which is about the same order as those for various crystals growing from liquid solution (Nyvlt et al., 1985) and from the vapor (Bennema and Leeuwen, 1975). They were linear with supersaturation and solubility, in agreement with Eq. 11, as shown in Figure 8. From the slope of the straight line in the figure, the value of βK_a was determined to be 3.6×10^{-3} mol/m^2·s. Linear correlation between growth rate and supersaturation due to the mechanism of corner nucleation was seldom reported in the literature. Instead, it was conventionally interpreted in terms of the linear law of spiral growth (Burton et al., 1951). Corner nucleation differs from spiral growth in that the former generates growth layers at the corners of a crystal face by two-dimensional nucleation, while the latter generate spiral dislocations, usually in the central region of the crystal face. Also, the proportionality of the growth rate with solubility has never been reported for crystal growth from a liquid solution. For growth from supercritical fluids, solubility can be varied independently at a constant temperature so that its effect on growth rate can be studied. However, this is not the case for growth from a liquid solution, where solubility can only be adjusted by changing the temperature, and its effect on growth rate cannot be determined without the interference of temperature effect.

The growth rates of the lateral (110) faces of the plates were also measured in this study. The measurement was performed with the basal faces parallel to the solution flow, but without exactly controlling the orientation of the (110) faces. One plate convenient for study was chosen arbitrarily for measurement even though there were several sprouted plates. The growth rates were constant as long as they grew stably, but decreased suddenly when unstable growth appeared. The measurement of the constant growth rates was easily done at low and moderate supersaturation when the growth stayed stable for a long time. However, the measurement of stable growth at high supersaturation can be performed only during a short period because unstable growth takes over after a short time. Growth rate data were taken at 83.6 bar only because difficulties were encountered at other levels of pressure. The growth rates of the stably growing (110) faces varied from 1.1×10^{-8} to 2.9×10^{-6} m/s as supersaturation varied from 0.044 to 0.31. They increased with supersaturation by a power of 2.5. This strongly nonlinear correlation implies that a bulk-diffusion barrier might be unimportant. In addition, a high power of 2.5 implies that spiral growth cannot be the case here, or the power would lie between 1 and 2. Thus Eq. 10 was applied and found to correlate the data well, as shown in Figure 9. From the slope of the straight line in the figure, the edge free energy γ was determined to be 1.8×10^{-21} J per molecule or equivalent to 5.6×10^{-3} J/m^2, a value lower than the interfacial tension of 0.02 J/m^2 suggested by Debenedetti (1990) for organic crystals nucleated from supercritical CO_2 solution.

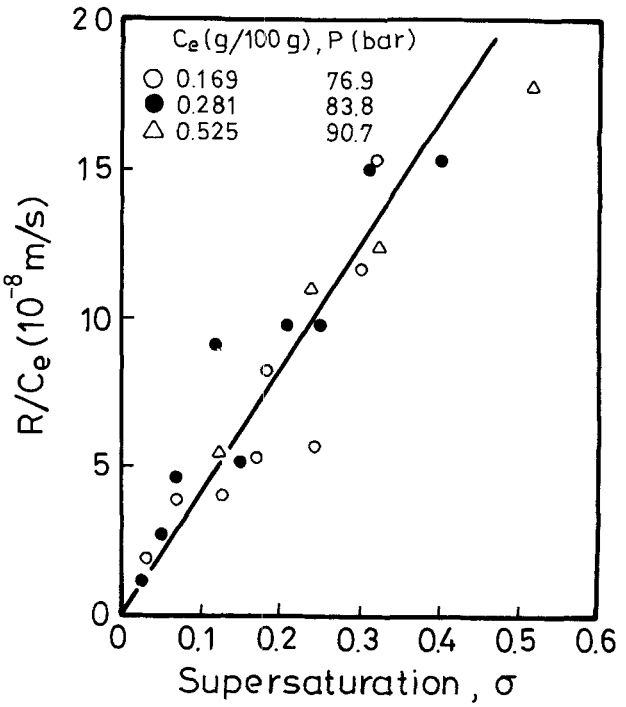

Figure 8. Effects of supersaturation and solubility on the growth rates of the (001) faces of the individuals at 318 K with solution velocity of 2.4×10^{-4} m/s.

Comparison of crystal growth from supercritical fluids, liquid solution, and vapor phase

The growth phenomena for naphthalene crystals from a supercritical CO_2 solution, that is, the development of individu-

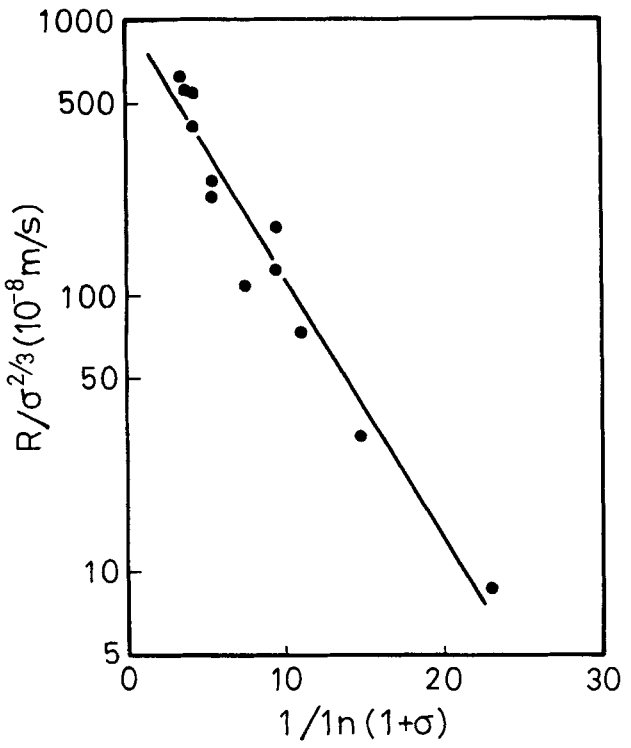

Figure 9. Effect of supersaturation on the growth rates of the lateral (110) faces of the sprouted plates at 318 K and 83.8 bar with a solution velocity of 2.4×10^{-4} m/s.

als, the sprouting of plates, the occurrence of hopper growth, and the stepped structure on the plates, are not unique. Similar observations have been reported for crystal growth both from a liquid solution and from the vapor phase. Examples are numerous in the literature: the development of individuals was found on spherical potash alum crystals growing from an aqueous solution (Buckley, 1951) and on spherical ice crystals from the vapor (Gliki et al., 1963); the sprouting of plates from a seed was seen on perovskite crystals growing from an aqueous solution (Mischgofsky, 1978) and on ice crystals from the vapor (Nakaya, 1954); the hopper growth was reported for many crystals growing from a liquid solution and from the vapor phase (Simov, 1976); the characteristics of the stepped basal faces were observed on the naphthalene plates nucleated from ethanol solution in our laboratory and on the ice plates from vapor phase (Nakaya, 1954).

As to the surface integration mechanism, generally, a transitional supersaturation exists below which crystals grow by the spiral mechanism and above by the mechanism of two-dimensional nucleation (Sunagawa, 1981). The transitional supersaturation depends on the edge free energy of a crystallization system; the larger edge free energy results in higher transitional supersaturation. Usually the transitional supersaturation is much larger in vapor growth than in solution growth because of the larger edge free energy in vapor growth (Lewis, 1980). For this reason, two-dimensional nucleation is seldom found on crystals growing from the vapor at low supersaturation, but has been reported for the growth of crystals from a liquid solution. For example, two-dimensional nucleation was negligible at supersaturation below 1.0 for the

Table 2. Comparison of Edge Free Energy for Crystal Growth from Supercritical CO_2 Solution, Liquid Solution, and Vapor

Crystal	Growth Medium	γ/kT	Reference
Naphthalene (110)	Supercritical CO_2 solution	0.41	This work
Octacosane (110)	Petroleum ether solution	0.2	Boistelle and Doussoulin (1976)
Hexatriacontane (110)	Petroleum ether solution	0.9*	Bourne and Davey (1976)
Hexamethylene tetramine	Ethanol solution	1.3*	Bourne and Davey (1976)
Hexamethylene tetramine	Aqueous solution	0.03*	Bourne and Davey (1976)
Sucrose	Aqueous solution	0.5	Bennema (1968)
Potassium alum	Aqueous solution	0.14	Bennema (1967b)
Sodium chlorate	Aqueous solution	0.2	Bennema (1967b)
Hexamethylene tetramine	Vapor	6*	Bourne and Davey (1976)
Monoclinic carbon tetrabromide	Vapor	12	Morgan and Dunning (1970)

*Edge energy is assumed approximately equal to edge free energy.

growth of naphthalene, phosphorus, and iodine crystals from the vapor (Lewis, 1974), but was found on *m*-chloronitrobenzene crystals growing from *o*-chloronitrobenzene solution at supersaturation of 0.04 (Murata and Honda, 1977) and on crystals of ammonium dihydrogen phosphate from an aqueous solution at supersaturation of 0.027 (Chernov, 1984). Therefore, the finding of two-dimensional nucleation at the face corners at supersaturation as low as 0.028 in this study leads us to conclude that the growth of naphthalene crystals from supercritical CO_2 solution resembles that of crystals from a liquid solution. The same conclusion also results from a comparison of edge free energy γ in Table 2. The values of edge free energy for naphthalene growing from supercritical CO_2 solution and for several crystals growing from a liquid solution are of the same order but about one order lower than those for crystals growing from the vapor.

The growth rates of naphthalene crystals from supercritical CO_2 solution depart, by an order of 5, from the theoretical rates calculated by using the linear law for vapor growth (Burton et al., 1951), as shown in Table 3. In applying the linear law, that is,

$$R = \beta\omega P_0(2\pi mkT)^{-1/2}\sigma$$
$$= \beta\Omega C_0(kT/2\pi m)^{1/2}\sigma, \qquad (13)$$

Table 3. Comparison of Growth Rates, Experimental vs. Theoretical (Eq. 13) of Naphthalene Crystals Growing from Supercritical CO_2 Solution at 45°C

Pres. (bar)	C_0 (mol/m^3)	R/σ (Theoretical) (10^{-3} m/s)	R/σ (Exp.) (10^{-8} m/s)
76.9	2.9	9.1	6.8
83.8	5.9	19	11
90.7	14	44	21

Table 4. Comparison of βK_a for Crystal Growth from Supercritical CO_2 and Aqueous Solution

Crystal	Growth Medium	Temperature (°C)	βK_a (10^{-4} mol/m^{2}s)	Reference
Naphthalene (001)	Supercritical CO_2 solution	45	36	This work
Sodium chlorate	Aqueous solution	30	26	Takeuchi et al. (1979)
Potassium chloride	Aqueous solution	41.5	9.2	Haneveld (1971)
Magnesium sulfate	Aqueous solution	16	4.5	Tai and Lin (1987)

where P_0 is the vapor pressure of the crystallizing compound, and C_0 the corresponding concentration, a value of 0.5 for β (Burton et al., 1951) has been used. The great difference between the experimental and theoretical rates implies that the two processes, growth from supercritical CO_2 solution and from the vapor, are entirely unlike.

The value of βK_a for naphthalene crystals growing from supercritical CO_2 solution is compared with the values for several salts grown from an aqueous solution in Table 4. In this table, Eq. 11 has been used to interpret the growth rate data, which are linearly correlated with supersaturation under a negligible bulk-diffusion barrier. Equation 11 is not specific for corner nucleation, but actually represents the limiting growth rate of a crystal face on which the surface-diffusion barrier is not important due to high step density, no matter what mechanism the steps result from. The value of βK_a for naphthalene is roughly the same order as the values for the salts, but a little bit larger. This implies that the adsorption-barriers in the two processes, growth from supercritical CO_2 solution and from an aqueous solution, are about the same order. The barrier for the naphthalene system is very likely due to the need for the solute molecules to desolvate from supercritical carbon dioxide, as the salt molecules generally do from water in an aqueous solution (Bennema, 1967a). This deduction is supported by the finding that a naphthalene molecule in supercritical CO_2 solution is surrounded by a CO_2 cluster of about 80 molecules (Kim and Johnston, 1987). Thus de-solvation must be important for the growth of naphthalene crystals from supercritical CO_2 solution. The slightly larger value of βK_a for naphthalene in supercritical CO_2 solution than the values for salts in an aqueous solution is understandable because the smaller solvation strength of solute in the supercritical solution is expected.

Conclusion

The growth phenomena, mechanism, and kinetics of naphthalene crystals from supercritical CO_2 solution were explored and compared with those from a liquid solution and vapor phase. Several growth features were observed: individuals bounded by facets developed from the seeds and a few of the individuals sprouted plates; the individuals underwent hopper growth as they grew larger; the plates were characteristic of one stepped and one smooth basal face, and sometimes grew unstably to become zigzag or dendritic. As for growth mechanism, the surface integration of the (001) faces of the individuals and that of the lateral (110) faces of the plates proceeded by two-dimensional nucleation at face corners and then followed by spreading the nuclei. Besides, the bulk-diffusion barrier was unimportant for the plates and for the individuals at small size. As to growth kinetics, the measured growth rates of the (001) faces of the individuals increased linearly with supersaturation and solubility, and those of the lateral (110) faces of the plates increased exponentially with supersaturation. Both of these observations were consistent with the theoretical findings for the corner nucleation mechanism.

Compared with the conventional processes of crystal growth, the growth of naphthalene crystals from supercritical CO_2 solution shows characteristics in growth mechanism and kinetics that are similar to liquid-solution growth but not to vapor growth, although the growth has many similarities in growth phenomena to both liquid-solution growth and vapor growth.

Acknowledgment

The authors gratefully acknowledge the financial support of the National Science Council of the Republic of China through grant NSC 79-0402-E002-19.

Notation

a = parameter in Eq. 12
A = area of a crystal face, m^2
b = parameter in Eq. 12
k = Boltzmann's constant, J/K
K = growth rate constant, m/s
m = weight of a molecule, kg
n_e = equilibrium concentration of adsorbed solute, mol/m^2
ω = volume of a molecule in crystal, m^3

Literature Cited

Bennema, P., "Analysis of Crystal Growth Models for Slightly Supersaturated Solutions," *J. Cryst. Growth*, **1**, 278 (1967a).
Bennema, P., "Interpretation of the Relation Between the Rate of Crystal Growth from Solution and the Relative Supersaturation at Low Supersaturation," *J. Cryst. Growth*, **1**, 287 (1967b).
Bennema, P., "Surface Diffusion and the Growth of Sucrose Crystals," *J. Cryst. Growth*, **3/4**, 331 (1968).
Bennema, P., and C. van Leeuwen, "Crystal Growth from the Vapor Phase: Confrontation of Theory with Experiment," *J. Cryst. Growth*, **31**, 3 (1975).
Berends, E. M., O. S. L. Bruinsma, and G. M. van Rosmalen, "Nucleation and Growth of Fine Crystals from Supercritical Carbon Dioxide," *J. Cryst. Growth*, **128**, 50 (1993).
Boistelle, R., and A. Doussoulin, "Spiral Growth Mechanisms of the (110) Faces of Octacosane Crystals in Solution," *J. Cryst. Growth*, **33**, 335 (1976).
Bourne, J. R., and R. J. Davey, "The Role of Solvent-Solute Interactions in Determining Crystal Growth Mechanisms from Solution, I. The Surface Entropy Factor," *J. Cryst. Growth*, **36**, 278 (1976).
Buckley, H. E., *Crystal Growth*, Wiley, New York (1951).
Burton, W. K., N. Cabrera, and F. C. Frank, "The Growth of Crystals and the Equilibrium Structure of Their Surfaces," *Phil. Trans. R. Soc. London*, **243**, 299 (1951).
Chernov, A. A., *Modern Crystallography: III. Crystal Growth*, Springer-Verlag, Berlin (1984).

Chernov, A. A., "Application of the Method of Characteristics to the Theory of the Growth Forms of Crystals," *Sov. Phys. Crystallog.*, **8**, 401 (1964).
Debenedetti, P. G., "Homogeneous Nucleation in Supercritical Fluids," *AIChE J.*, **36**, 1289 (1990).
Gliki, N. V., A. A. Eliseev, and N. M. Marchenko, "The Growth of Spherical Ice Crystals," *Sov. Phys. Crystallog.*, **7**, 488 (1963).
Haneveld, H. B. K., "Growth of Crystals from Solution: Rate of Growth and Dissolution of KCl," *J. Cryst. Growth*, **10**, 111 (1971).
Kelley, F. D., and E. H. Chimowitz, "Experimental Data for the Crossover Process in a Model Supercritical System," *AIChE J.*, **35**, 981 (1989).
Kim, S., and K. P. Johnston, "Clustering in Supercritical Fluid Mixtures," *AIChE J.*, **33**, 1603 (1987).
Krukonis, V. J., "Supercritical Fluid Nucleation of Difficult-to-Comminute Solids," AIChE meeting, San Francisco (Nov., 1984).
Larson, K. A., and M. L. King, "Evaluation of Supercritical Fluid Extraction in the Pharmaceutical Industry," *Biotechnol. Prog.*, **2**, 73 (1986).
Lewis, B., "The Growth of Crystals at Low Supersaturation, II. Comparison with Experiment," *J. Cryst. Growth*, **21**, 40 (1974).
Lewis, B., "Nucleation and Growth Theory," in *Crystal Growth*, B. R. Pamplin, ed., Pergamon, New York (1980).
Mischgofsky, F. H., "Face Stability and Growth Rate Variations of the Layer Perovskite $(C_3H_7NH_3)_2CuCl_4$," *J. Cryst. Growth*, **44**, 223 (1978).
Mohamed, R. S., P. G. Debenedetti, and R. K. Prud'homme, "Effects of Process Conditions on Crystals Obtained from Supercritical Mixtures," *AIChE J.*, **35**, 325 (1989).
Morgan, A. E., and W. J. Dunning, "The Growth of Monoclinic Carbon Tetrabromide Crystals," *J. Cryst. Growth*, **7**, 179 (1970).
Murata, Y., and T. Honda, "The Growth of *m*-Chloronitrobenzene Crystals," *J. Cryst. Growth*, **39**, 315 (1977).
Nakaya, U., *Snow Crystals*, Harvard Univ. Press, Cambridge, MA (1954).
Nyvlt, J., O. Sohnel, M. Matuchova, and M. Broul, *The Kinetics of Industrial Crystallization*, Elsevier, New York (1985).
Paulaitis, M. E., V. J. Krukonis, R. T. Kurnik, and R. C. Reid, "Supercritical Fluid Extraction," *Rev. Chem. Eng.*, **1**, 179 (1983).
Shaub, G. R., J. F. Brennecke, and M. J. McCready, "Flow Field Effects on Particles Formed from the Rapid Expansion of Supercritical Fluid Solutions," *Proc. 2nd Int. Symp. Supercritical Fluids*, Boston, p. 338 (1991).
Simov, S., "Morphology of Hollow Crystals of II–VI Compounds," *J. Mater. Sci.*, **11**, 2319 (1976).
Strickland-Constable, R. F., *Kinetics and Mechanism of Crystallization*, Academic Press, London (1968).
Sunagawa, I., "Characteristics of Crystal Growth in Nature as Seen from the Morphology of Mineral Crystals," *Bull. Mineral.*, **104**, 81 (1981).
Tai, C. Y., and C. Lin, "Crystal Growth Kinetics of the Two-Step Model," *J. Cryst. Growth*, **82**, 377 (1987).
Tai, C. Y., C. Cheng, and Y. Huang, "Interpretation of Crystal Growth Rate Data Using a Modified Two-step Model," *J. Cryst. Growth*, **123**, 236 (1992).
Takeuchi, H., K. Takahashi, K. Tomita, and M. Imanaka, "Growth Rate and Size Distribution of $NaClO_3$ Crystals from Aqueous Solution," *J. Chem. Eng. Japan*, **12**, 209 (1979).
Tavana, A., and A. D. Randolph, "Manipulating Solids CSD in a Supercritical Fluid Crystallizer: CO_2-Benzoic Acid," *AIChE J.*, **35**, 1625 (1989).
Tom, J. W., and P. G. Debenedetti, "Particle Formation with Supercritical Fluids—A Review," *J. Aerosol. Sci.*, **22**, 555 (1991).
Tsekhanskaya, Yu. V., M. B. Iomtev, and E. V. Mushkina, "Solubility of Naphthalene in Ethylene and Carbon Dioxide Under Pressure," *Russ. J. Phys. Chem.*, **38**, 1173 (1964).
Wells, A. F., "Crystal Habit and Internal Structure," *Phil. Mag.*, **37**, 184 (1946).

Manuscript received May 31, 1994, and revision received Nov. 8, 1994.